Climate Variability Inferred from a Layered Model of the Ventilated Thermocline*

RUI XIN HUANG AND JOSEPH PEDLOSKY

Department of Physical Oceanography, Woods Hole Oceanographic Institution, Woods Hole, Massachusetts

(Manuscript received 19 February 1998, in final form 2 June 1998)

ABSTRACT

Climate variability of a layered model of the ventilated thermocline is studied. Assuming the Ekman pumping is unchanged, cooling (heating) causes a southward (northward) shift of the outcrop line and thus induces a baroclinic response in the ventilated thermocline. The perturbations propagate within a characteristic cone downstream from the cooling (heating) region, defined by the two outermost characteristics streaming from the edge of the cooling (heating) region.

Changes in Ekman pumping rate induce a barotropic response that propagates westward, which is a classic result obtained from the Sverdrup relation. However, if the outcrop line is nonzonal, there can be an additional baroclinic response, which propagates within the characteristic cone downstream from the source region of an Ekman pumping anomaly.

1. Introduction

Theories of the thermocline have been one of the major challenges in our field. Although theories evolved gradually over the past decades, many pressing questions remain. For example, what is the thermocline variability in response to climate variability? Due to the complicated and nonlinear nature of the oceanic dynamics, a complete answer to this question remains a great challenge.

A major obstacle on the road to understand the thermocline variability is the strong waves excited by changes in surface forcing due to Ekman pumping and cooling/heating. Although many studies have been devoted to examine the thermocline variability associated with wave activity, we do not seem to have simple solutions for this problem.

Difficulties associated with transient, wavelike responses to short-term forcing can be minimized when we deal with longer-term climatic variations. If the timescale for such variations is long compared to the transit time of baroclinic Rossby waves through the gyre, about a decade, we can consider the ocean in quasi equilibrium with the forcing. In such cases the thermocline anomaly associated with the variability can be identified as the difference between the steady states associated with a ''standard'' forcing and the solution state determined by the anomalous forcing. The difference, not necessarily small, is a snapshot of the thermocline variability (at very low frequency).

The ease with which the thermocline variability can be calculated is the advantage of this point of view. The drawback is that the wave processes associated with the setup of the anomalous state are ignored. We feel that the very clear pattern of anomaly that emerges from the quasi-steady approach compensates for the incompleteness of our approach. However, the reader must keep in mind that not all of the variability is captured by our quasi-steady solution.

In addition, we will assume that the basic stratification of the ocean remains unchanged within the decadal timescale. In the ventilated thermocline theory the wind-driven circulation is treated as a perturbation to the background stratification set up by the external thermohaline circulation. Thus, specifying the background stratification is one of the preconditions of the theory.

2. Thermocline variability inferred from a two-layer model

Our study of the thermocline variability in response to climate change is based on the simple layered model of the ventilated thermocline (Luyten et al. 1983, LPS hereafter). We begin with the simplest version, in which there are only two moving layers and the lower layer outcrops along a line $f_2(x)$, Fig. 1. The upper-layer thickness is h_1, and the lower layer h_2. The total depth of the ventilated layer is $H = h_1 + h_2$. North of the

* Woods Hole Oceanographic Institution Contribution Number 9697.

Corresponding author address: Dr. Rui Xin Huang, Dept. of Physical Oceanography, Woods Hole Oceanographic Institution, Woods Hole, MA 02543.
E-mail: huang@dragon.whoi.edu

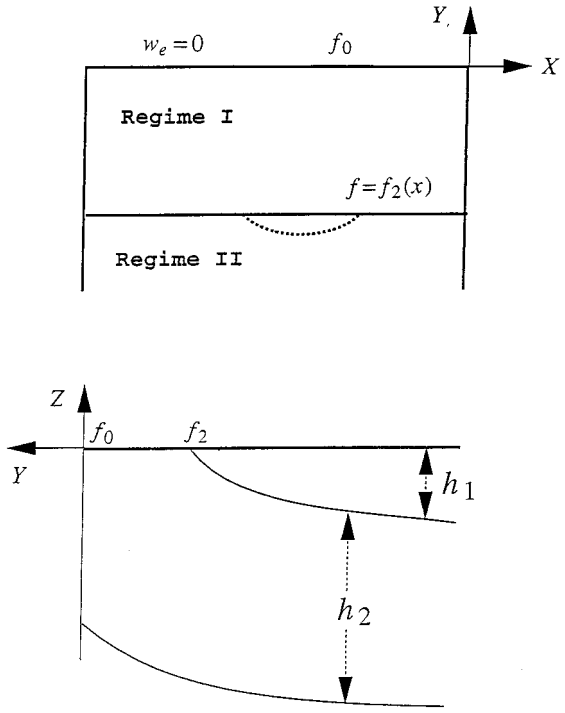

FIG. 1. Schematic structure of the ventilated thermocline with two moving layers.

outcrop line (Regime I), there is only one moving layer, layer 2. Circulation in this regime is described by a simple reduced gravity model, so the layer depth satisfies

$$H^2 = h_2^2 = D_0^2(x, y) + H_e^2, \tag{1}$$

where H_e is the thickness of layer 2 along the eastern boundary,

$$D_0^2(x, y) = -\frac{2f^2}{\gamma_2\beta}\int_x^{x_e} w_e\, dx' \tag{2}$$

is a given function determined by the Ekman pumping field, $\gamma_n = g(\rho_{n+1} - \rho_n)/\rho_0$ and ρ_0 is the average density of the thermocline water, $\beta = df/dy$, x_e is the eastern boundary of the model ocean, and w_e is the Ekman pumping.

Along the given outcrop line, the layer thickness is a given function of the x coordinate, $H = H_{00}(x)$. By inverting this function, we have a function $f_2 = f_2(H)$, which is valid along the outcrop line.

South of the outcrop line (Regime II), there are two moving layers. The dynamics in this regime is well known from the ventilated thermocline theory. The essential point is that potential vorticity in the second layer is conserved along streamlines, which is the same as the isodepth line $H = \text{const}$. Thus, layer thicknesses in this regime satisfy

$$h_2 = \frac{f}{f_2(H)}H, \qquad h_1 = \left(1 - \frac{f}{f_2(H)}\right)H. \tag{3}$$

The zonal integration of the Sverdrup relation is (see LPS for details)

$$H^2 + \frac{\gamma_1}{\gamma_2}h_1^2 = D_0^2 + H_e^2. \tag{4}$$

Substituting (3), one obtains

$$H^2\left[1 + \frac{\gamma_1}{\gamma_2}\left(1 - \frac{f}{f_2(H)}\right)^2\right] = D_0^2 + H_e^2. \tag{5}$$

If the outcrop line is along a latitudinal circle, f_2 is constant. Thus, the ratio of layer thicknesses in the ventilated zone only depends on the latitude. The solution for such a simple case has been discussed in detail by LPS.

a. Response to cooling/heating

If the climate changes, we suppose that the surface of the ocean will be heated or cooled by the atmosphere. This may be represented in the LPS model as a displacement of the outcrop line separating cool and warm water. Thus if the ocean is locally cooled (heated), the outcrop line, $f = f_2$, will be locally moved southward (northward). Although this change may be of arbitrary magnitude, it is illuminating to first consider the case where the position of the outcrop line is only slightly perturbed. If f_2 is the constant value of the outcrop line in the absence of a cooling or heating anomaly, we write the anomalous position of the outcrop line as $f_{\text{outcrop}} = f_2 + \delta f(x)$. Along this perturbed outcrop line the total layer depth satisfies

$$H_2^2 = -\frac{2f_{\text{outcrop}}^2(x)}{\gamma_2\beta}\int_x^{x_e} w_e(x', y)\, dx' + H_e^2. \tag{6}$$

It is readily shown that

$$H_2^2(x) = H_{20}^2(x) + O(\delta f), \tag{7}$$

where $H_{20}(x)$ is the total layer thickness along the unperturbed outcrop line. Thus, to the first-order approximation, the functional relation between H and x remains unchanged. It is readily shown that the inversion leading to $f = f(H)$ along the outcrop line yields

$$f_2(x(H)) = f_2 + \delta f(H_0) + O(\delta f)^2. \tag{8}$$

The corresponding equation for the total depth is now

$$H^2\left[1 + \frac{\gamma_1}{\gamma_2}\left(1 - \frac{f}{f_2 + \delta f}\right)^2\right] = D_0^2 + H_e^2. \tag{9}$$

In the form given in (9), which is identical to (5), δf could be of any magnitude and the solution of (9) could proceed numerically. However, it is useful to exploit (8) in the case of small δf. For $\delta f \ll f$, we have

$$H^2 = (D_o^2 + H_e^2)\left\{1 + \frac{\gamma_1}{\gamma_2}\left(1 - \frac{f}{f_2}(1 - f\delta f/f_2)\right)^2\right\}^{-1}$$

$$\approx H_0^2\left[1 - \frac{2\frac{\gamma_1}{\gamma_2}(1 - f/f_2)\frac{f\delta f}{f_2^2}}{1 + \frac{\gamma_1}{\gamma_2}(1 - f/f_2)^2}\right], \quad (10)$$

where

$$H_0^2 = \frac{D_0^2 + H_e^2}{1 + \frac{\gamma_1}{\gamma_2}(1 - f/f_2)^2} \quad (11)$$

is the square of the unperturbed total layer thickness. Thus, one obtains

$$H \approx H_0\left[1 - \frac{\frac{\gamma_1}{\gamma_2}(\mathbf{1} - \mathbf{f}/\mathbf{f_2})\frac{\mathbf{f}\delta\mathbf{f}}{\mathbf{f_2^2}}}{\mathbf{1} + \frac{\gamma_1}{\gamma_2}(\mathbf{1} - \mathbf{f}/\mathbf{f_2})^2}\right]. \quad (12)$$

Similarly, one has

$$h_1 \approx H_0\left[1 - \frac{\frac{\gamma_1}{\gamma_2}(1 - f/f_2)\frac{f\delta f}{f_2^2}}{1 + \frac{\gamma_1}{\gamma_2}(1 - f/f_2)^2}\right]\left[1 - \frac{f}{f_2} + \frac{f\delta f}{f_2^2}\right]$$

$$\approx H_0\left[1 - \frac{f}{f_2} + \frac{\mathbf{f}\delta\mathbf{f}}{\mathbf{f_2^2}}\frac{\mathbf{1}}{\mathbf{1} + \gamma_1/\gamma_2(\mathbf{1} - \mathbf{f}/\mathbf{f_2})^2}\right]; \quad (13)$$

$$h_2 = H - h_1 \approx H_0\frac{f}{f_2}\left\{1 - \frac{\frac{\gamma_1}{\gamma_2}(\mathbf{1} - \mathbf{f}/\mathbf{f_2}) + \mathbf{1}}{\mathbf{1} + \frac{\gamma_1}{\gamma_2}(\mathbf{1} - \mathbf{f}/\mathbf{f_2})^2}\frac{\delta\mathbf{f}}{\mathbf{f_2}}\right\}. \quad (14)$$

In Eqs. (12)–(14), the thickness perturbations are in bold face.

In the case of cooling, the outcrop line moves southward. Since $\delta f < 0$, both h_2 and H increase, while h_1 decreases. From (12) and (14),

$$\frac{\delta h_2}{\delta H} = \frac{2f_2 - f}{f_2 - f};$$

thus, δh_2 is much larger than δH. Although δH is much smaller than δh_2, it is positive. Accordingly, cooling at the surface cause the lower isopycnal surface to move downward, and this leads to warming of the lower part of the thermocline. The downward displacement induced by cooling on the surface can be interpreted as follows. Cooling the upper ocean reduces the equivalent density stratification. In term of a simple reduced-gravity model, weaker stratification leads to a deeper thermocline.

It is important to recall that δf in the above formulas is a function of H_0; thus, it is different from zero everywhere in the fluid south of the outcrop line where H_0 takes those values that on the outcrop line render δf different from zero. That is, the perturbation propagates away from the outcrop line on the characteristics $H =$ const and in the slightly perturbed problem these lines are known from the outset and occupy the zone between the two streamlines that serve as ''bookends'' along the outcrop line for the perturbation.

Our analysis above indicates that in the case of cooling there is a baroclinic response in the thermocline. Since the perturbation is propagated along characteristics, this perturbation is confined within the characteristic cone defined by the two outermost characteristics streaming from the edge of the cooling region.

We have set up a simple two-layer model in spherical coordinates, with a southern boundary at $\theta_s = 20°$N and a northern boundary at $\theta_n = 50°$N. The model basin is 60° wide, mimicking the Atlantic. The second-layer thickness along the eastern boundary is set to 670 m, and $\gamma_1 = \gamma_2 = 1$ cm s^{-2}. The outcrop line is originally half-way between the southern and the northern boundary. The model is forced by an Ekman pumping

$$w_e = -0.0001 \sin\left(\pi\frac{\theta - \theta_s}{\theta_n - \theta_s}\right) \text{ cm s}^{-1}. \quad (15)$$

Assuming a regional cooling, the meridional perturbation of the outcrop line is

$$\delta y = \begin{cases} \Delta y\sqrt{1 - (x - x_0)^2/r_0^2}, & |x - x_0| \le r_0 \\ 0, & |x - x_0| \ge r_0, \end{cases} \quad (16)$$

where x_0 and r_0 is the longitudinal position and the radius of the ellipse and Δy is the maximum meridional displacement of the outcrop line. Given the perturbation of the outcrop line, changes in the thermocline can be calculated accordingly. There is clearly a baroclinic response to the cooling shown in Fig. 2, and the perturbations are confined within the characteristic cone originating from the outer edge of the cooling source region. Within this characteristic cone, the upper layer becomes thinner, and the lower layer becomes thicker. The upper part of thermocline is cooled, that is, the amount of warm water is reduced while the thickness of the cold layer is increased. However, the lower part of the thermocline is slightly warmed up because the lower interface actually moves downward, as shown in the lower panel of Fig. 2. For this case the maximum southward migration of the outcrop line is $\Delta y = 3.5°$. The upper interface rises about 60 m, which is a fairly large vertical movement. Note that the interfacial displacement gradually declines toward south; however, the total depth of the ventilated thermocline keeps increasing southward. The layer thickness changes imply a baroclinic velocity anomaly. In the upper layer, the velocity anomaly tends to intensify the southwestward velocity in the lower half of the characteristic cone, and it reduces the south-

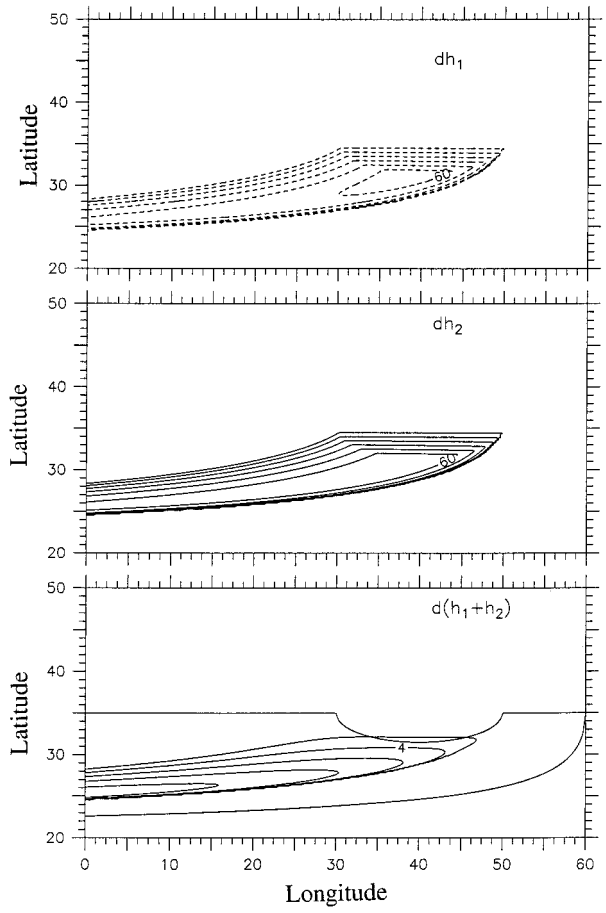

FIG. 2. Perturbations in layer thickness (m) in response to a regional cooling ($\Delta y = -3.5°$), represented by a southward migration of the outcrop line, as indicated by the thin line in the lowest panel.

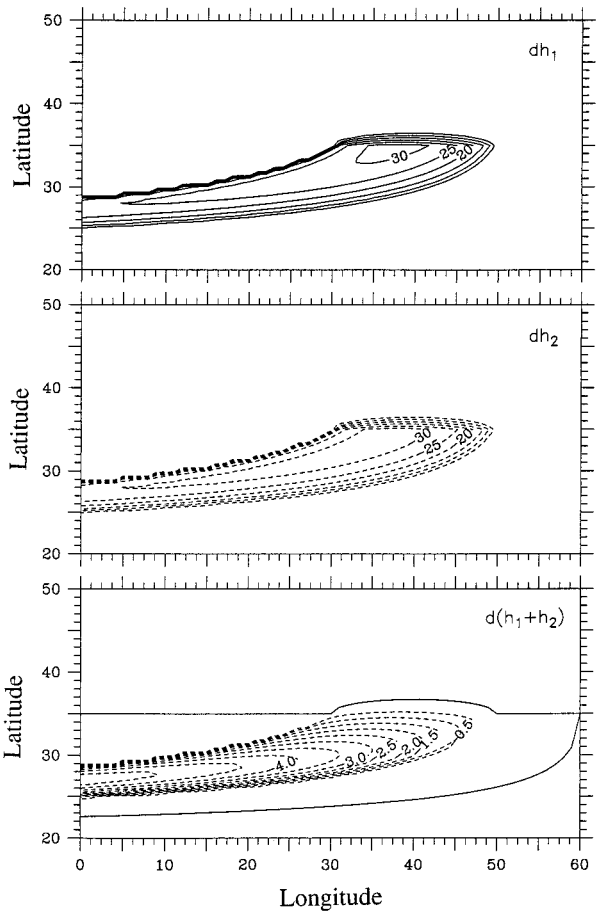

FIG. 3. Perturbations in layer thickness (m) in response to a regional heating ($\Delta y = 1.75°$), represented by a northward migration of the outcrop line, as indicated by the thin line in the lowest panel.

westward velocity in the upper half of the characteristic cone. Velocity changes in the lower layer have an opposite sign.

When there is a warm anomaly, the outcrop line moves poleward. A typical solution is shown in Fig. 3. There is a clear baroclinic response to the warming, and the sign of the thermocline anomaly is opposite to that of cooling. Once again, the perturbations propagate downstream and are confined by two outermost characteristics originated from the source of warming.

Our numerical calculations show that as long as the perturbation is small, the linear perturbation solution is a very good approximation to the fully nonlinear solution. For example, when the meridional migration of the outcrop line is less than 3 deg, the linear perturbation solution differs from the fully nonlinear solution by less than 1%–2%.

When the slope of the outcrop line is too large, there may not be a consistent solution for the ventilated thermocline. As shown in Fig. 4, when the outcrop line's slope exceeds that of the local streamline in layer 2, there may not be a consistent solution for the model, unless the potential vorticity at points **A** and **B** happen to have the same value. Since there are an infinite numbers of points along this segment of the outcrop line, this consistent constraint has to be satisfied for any pair

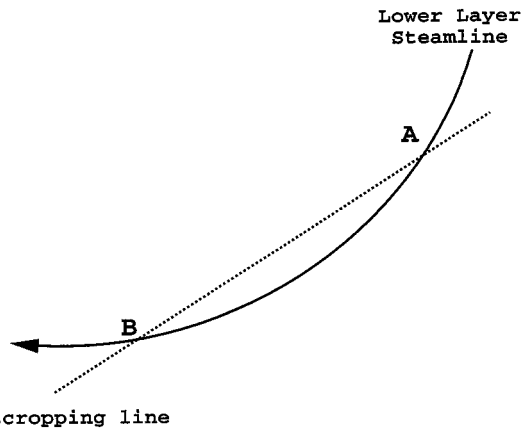

FIG. 4. Barotropic streamlines and an outcrop line that may violate the potential vorticity conservation principle.

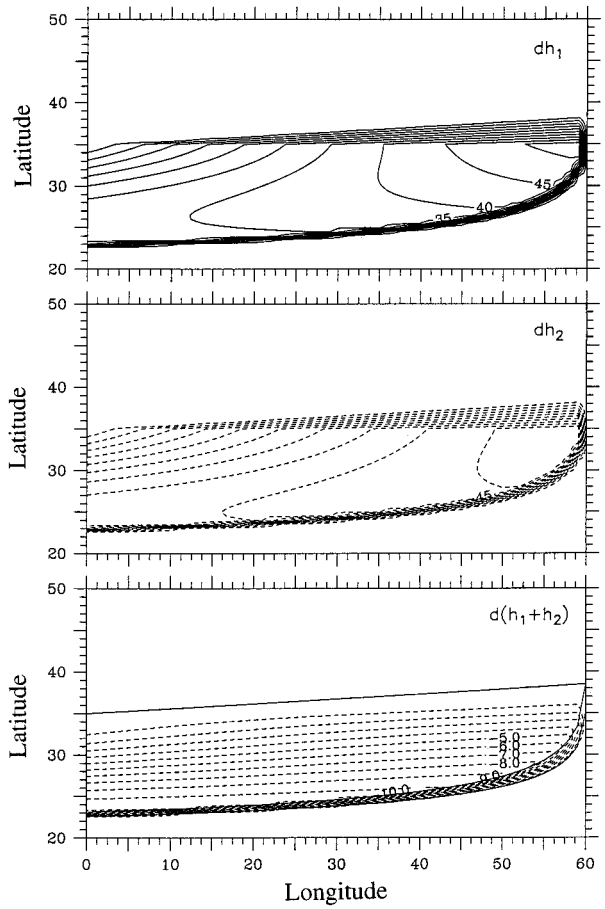

FIG. 5. Perturbations in layer thickness (m) in response to a warming in the eastern basin, represented by a poleward migration of the outcrop line, as indicated by the thin line in the lowest panel.

of points along this segment. Unless the model is subject to some rather strange constraints, such a consistent condition is unlikely to be met. Thus, the ventilated thermocline model may not work for such cases. The physical implication of such cases remains to be explored. In fact, if Δy is larger than 1.75°, the value chosen for the case presented in Fig. 3, no consistent solution can be find by our approach.

Another interesting case is when the eastern basin is warmed up. In this case the outcrop line moves poleward, as shown by the thin line in the lowest panel in Fig. 5. There is a basinwide baroclinic response. The upper layer becomes 40 m thicker, and the lower layer is 50 m thinner. The base of the moving layer moves upward about 5–10 m. Our two-layer model can be considered as a crude idealization of the continuously stratified oceans. Thus, when the upper interface in the layer model moves upward, an isopycnal in the upper part of the equivalent continuously stratified ocean moves upward. Thus, the upper ocean is warmed. Similarly, the lower part of the thermocline in the equivalent continuously stratified ocean is cooled.

Changes in the thermocline are advected to the western boundary where the perturbations will be advected both poleward and equatorward via the western boundary. Thus, warming in the eastern basin can affect other parts of the oceans through the mass redistribution via the western boundary. We speculate that warming of the southeastern basin can lead to cooling of the lower thermocline. Through the western boundary current the cooled lower thermocline water eventually goes upward through the regime of equatorial upwelling, and this may bring down the surface temperature in the southeastern basin. Thus, the baroclinic response to the warming or cooling may induce a decadal oscillation in the ocean. However, the detail of such a loop oscillator should be examined by using a model in which the time-dependent processes during the adjustment are explicitly included.

The poleward migration of the outcrop line induces major changes, especially within two zones. First, since the outcrop line moves northward, the ventilated zone expands northward. Within a narrow triangle strip along the northern edge of the outcrop line, the thermocline structure changes drastically because it now consists of two moving layers. Similarly, due to the migration of the outcrop line near the eastern boundary, the boundary of the shadow zone also moves northward. As a result, the circulation changes dramatically near the edge of the shadow zone. These sharp changes appear as two strips of strong perturbations along the northern and southern edges of the perturbation depth map, Fig. 5.

If the eastern basin is cooled while the western basin is warmed, the response is the combination of these two baroclinic modes. While cooling in the eastern basin induces a decline in the upper layer thickness, the warming in the western basin induces an increase in the upper-layer thickness, Fig. 6. The response in the lower layer is of opposite sign.

In the real oceans, a decadal cold anomaly and a warm anomaly may have rather complicated spatial patterns. Thus, the response of the thermocline is a combination of the baroclinic mode due to each patch of cooling/heating.

Although our discussion has been limited to the case of two moving layers only, a similar analysis can be extended to the case with three moving layers. In fact, we have also formulated a model with three moving layers. The problem is again reduced to either a perturbation solution of the case of an initially zonal outcrop line, or the fully nonlinear equation can be solved numerically. In the case of three moving layers, the perturbation of each outcrop line induces a baroclinic response that propagates within the characteristic cone downstream from the cooling/heating source.

The three-layer model does allow us to verify that if only the *southern* of the two outcrop lines is disturbed by local heating, the thickness of layer 2 increases as does the total depth while the thickness of layer 3 increases only slightly. This strengthens our previous heuristic extrapolation of the results of the two-layer model

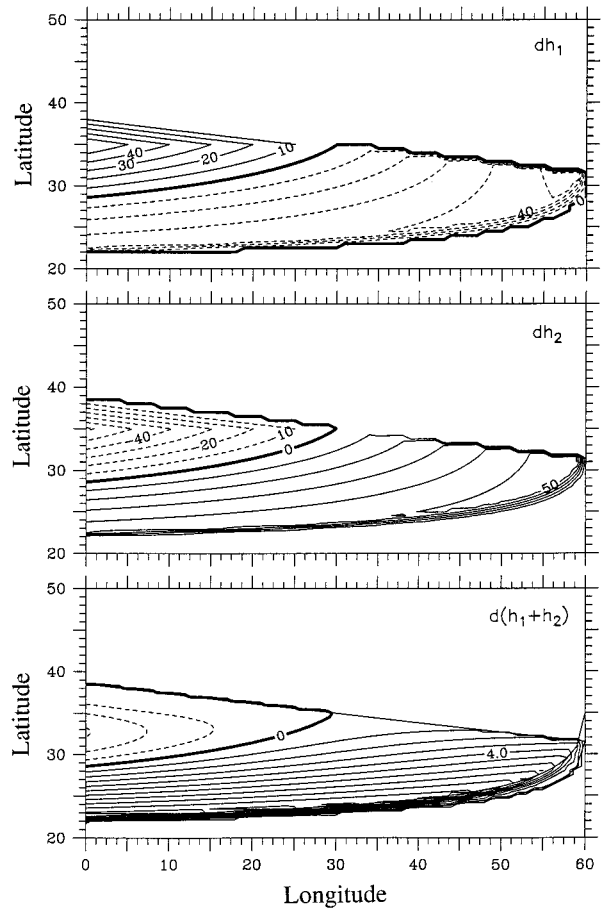

FIG. 6. Perturbations in layer thickness (m) in response to a warming in the western basin and cooling in the eastern basin, as indicated by the new outcrop line depicted by thin line in the lowest panel.

to the continuous model, that is, that local surface heating (cooling) can lead to a deep cooling (heating) of the thermocline. The three-layer model is discussed in more detail in section 3.

b. Response to changes in Ekman pumping

Assume that the outcrop line is defined as $f = f(x)$ and the Ekman pumping rate is $w_e = w_e(x, y)$. We now study changes in the thermocline structure in response to a perturbation in the Ekman pumping velocity, $w_e'(x, y)$. The total depth satisfies

$$H^2\left[1 + \frac{\gamma_1}{\gamma_2}\left(1 - \frac{f}{f_2'(x(H))}\right)^2\right] = D_0^2 + H_e^2, \quad (17)$$

where $f_2'(x(H))$ is the new functional relationship between layer thickness H and the Coriolis parameter under the new Ekman pumping rate $w_e + w_e'$. This nonlinear equation can be solved numerically.

Since our analysis here is based on the original LPS model, in which thermodynamics is excluded, we can only specify the outcrop line a priori. As the simplest choice, we will assume that the outcrop lines do not change, even if the Ekman pumping rate has been changed.

If instead, we imagine the case where an (unspecified) thermodynamic process specifies a priori an $f(H)$ relation, then (17) indicates that there would be no perturbation of the layer thicknesses south of the region of anomalous Ekman pumping. This includes the special case where $f(H)$ is purely zonal and equal to f_2. In such cases the response is strictly barotropic and the anomaly propagates purely westward. If the outcrop line is tilted, and remains in a fixed position as w_e changes, then a baroclinic response to the Ekman pumping variation is felt within the cone of characteristics propagating southwestward. We emphasize that this effect is absent in the LPS model, which fixes the outcrop lines as zonal.

Assume the total depth of the ventilated layers is H. The potential vorticity conservation constraint requires that the streamline in the second layer should be traced back to a new place $x + \delta x$ along the same outcrop line where the layer depth H under the forcing of $w_e + w_e'$ is equal to the layer depth at the old position x under the old forcing w_e:

$$\begin{aligned}\delta H^2 &= -\frac{2f_2^2(x + \delta x)}{\gamma_2\beta}\int_{x+\delta x}^{x_e}(w_e + w_e')\,dx \\ &\quad + \frac{2f_2^2(x)}{\gamma_2\beta}\int_x^{x_e} w_e\,dx \\ &\approx -\frac{2\alpha f_2(x)\delta x}{\gamma_2}\int_x^{x_e} w_e\,dx - \frac{2f_2^2(x + \delta x)}{\gamma_2\beta}\int_x^{x_e} w_e'\,dx \\ &\quad + \frac{2f_2^2(x + \delta x)}{\gamma_2}(w_e + w_e')\delta x. \end{aligned} \quad (18)$$

Note that we have used a relation between the Coriolis parameter and the x coordinate that is valid along the outcrop line:

$$f_2(x + \delta x) = f_2(x) + \beta\alpha\delta x, \quad (19)$$

where α is the slope of the outcrop line. Since the layer thickness at these two locations should be the same, $\delta H = 0$. Thus, to the lowest order approximation, the perturbation in location is

$$\delta x = \frac{f_2^2(x)\int_x^{x_e} w_e'\,dx}{f_2^2(x)w_e - \alpha\beta f_2(x)\int_x^{x_e} w_e\,dx}. \quad (20)$$

The second term in the denominator is generally smaller than the first term, so for a quantitative analysis, this term can be omitted. Thus, the meridional shift due to the shift in along-outcrop line position δx, is roughly equal to

$$\delta y = \frac{\alpha \int_x^{x_e} w_e' \, dx}{w_e}. \tag{21}$$

Assuming a negative slope α, an increase in the Ekman pumping rate gives rise to a negative δy. A negative δy means that for the same total layer depth the streamline in the second layer is now originated from a somewhat southward position along the outcrop line. As a result, the Coriolis parameter declines. Thus, there is a baroclinic response south of the source regime, similar to the case of cooling.

For the first case, the outcrop line is slightly tilted, starting from 38°N at the western boundary and intercepting the eastern boundary at 32°N at the eastern boundary. There is a patch of stronger Ekman pumping in the eastern basin, with its center at (35°N, 45°E). The magnitude of the Ekman pumping rate anomaly is -1.0×10^{-5} cm s^{-1}, and it linearly declines to zero at the edge of circle, whose radius is 6°.

There is clearly a barotropic response west of the Ekman pumping anomaly, as expected from the Sverdrup dynamics. The most important phenomenon is the baroclinic response, which propagates within the characteristic cone originated from the source of anomaly (Fig. 7). The upper layer becomes thinner and the lower layer becomes thicker in this characteristic cone. Thus, when the outcrop line is tilted from northwest to southeast, a stronger Ekman pumping can induce a baroclinic response in the thermocline, which has a similar structure within the characteristic cone as the cooling case described earlier. The major difference between cooling and Ekman pumping anomalies is the barotropic response west of the Ekman pumping anomaly. In both the southern parts of the North Atlantic and North Pacific, outcrop lines have orientations similar to the case discussed above. In fact, the slope of these outcrop lines can be even larger. Thus, the baroclinic response from Ekman pumping anomaly is about the same order as that due to cooling/heating.

As a second example, we present another case where the outcrop line is tilted SW–NE. Under a stronger Ekman pumping anomaly, there are both barotropic and baroclinic responses. The baroclinic response has a sign opposite to the previous case, Fig. 8. In the northern part of the North Atlantic and North Pacific, the outcrop lines have a general SW–NE orientation. Thus, a strong Ekman pumping anomaly there can induce a baroclinic response that resembles a local heating anomaly.

The analysis presented above is based on an assumption that the outcrop line does not change its position in response to the new Ekman pumping field. Such an assumption is an idealization, which may not represent the real physics.

Physically, the outcrop line may shift meridionally under the influence of Ekman pumping rate change. For example, in the southern part of the subtropical gyre, a positive westward wind anomaly can increase the Ekman pumping rate. However, stronger easterlies can transport more warm water from low latitudes and thus reduces the density in the mixed layer. As a result, the outcrop line tends to move poleward, Fig. 9. On the other hand, a stronger westerly in the northern part of the subtropical gyre can increase the Ekman pumping rate. More cold water can be brought from the north and density in the mixed layer can increase; then the outcrop line tends to move southward.

If the outcrop line moves to a new place, the functional relation $f(H)$ (along the outcrop line) will be changed. As a result, the response of the thermocline to changes in Ekman pumping may be different from the simplified solution discussed above. For example, if the Ekman pumping increases, at a given latitude each point of the outcrop line moves to a new place. As a special case, let us assume that the layer thickness at the new location is exactly the same as the layer thickness at the old position under the undisturbed Ekman pumping field. Thus, the functional relation $f_2(H)$ re-

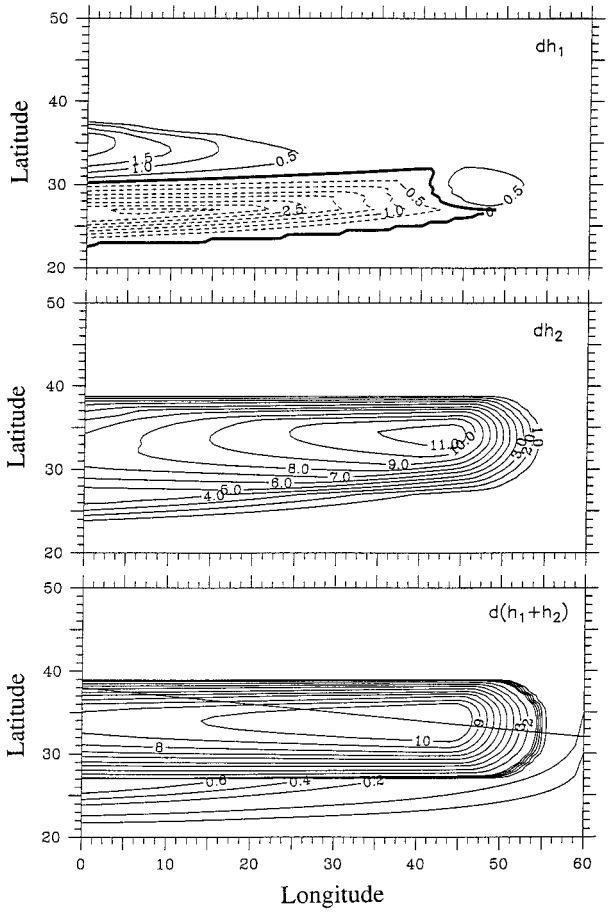

FIG. 7. Perturbations in layer thickness (m) in response to an increase of Ekman pumping, the outcrop line has a negative slope, as depicted by the thin line in the lowest panel.

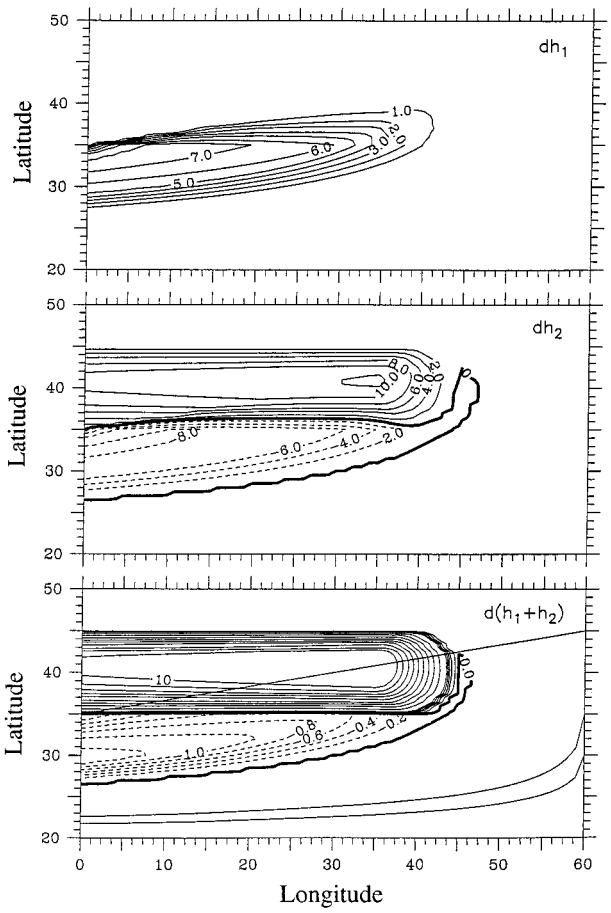

FIG. 8. Perturbations in layer thickness (m) in response to an increase of Ekman pumping, the outcrop line has a positive slope, as depicted by the thin line in the lowest panel.

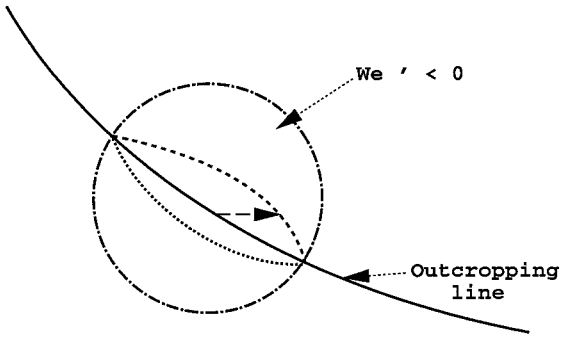

FIG. 9. Possible migration of the outcrop line in response to changes in Ekman pumping rate.

mains unchanged. A simple reasoning leads to a seemingly shocking result that there would be no perturbation within the characteristic cone. However, this is really no surprise because the baroclinic response due to the Ekman pumping anomaly and outcrop line movement exactly cancel each other, and only the barotropic response is retained. In a more realistic model, the outcrop line's position should be altered in response to the Ekman pumping anomaly. However, such a model is beyond the scope of our discussion in this study.

3. Thermocline variability inferred from a three-layer model

A two-layer model is a highly idealized case. With more layers added, the ventilated thermocline model becomes more realistic, but the model's behavior also becomes much more complicated. Since our primary goal in this note is to lay out the theoretical framework with minimal complexity, we chose a smaller third-layer thickness along the eastern boundary, $h_{3e} = 500$ m. This separates the affected ventilated zone and the shadow zone and simplifies the calculation. All other parameters remain the same as in the two-layer model, except there are now two outcrop lines. In the unperturbed state, the second layer outcrops along $y_2 = 42.5°$N and the first layer outcrops along $y_1 = 35°$N. Although one may find the perturbation solutions to the LPS model with three moving layers by an analytical approach, it is easier to find the solutions by solving the fully nonlinear equations numerically. Solutions presented here have been obtained by this numerical approach.

First, we examine the case of cooling within a small region along the southern outcrop line y_1 (the northern outcrop line y_2 remains unchanged), shown in the left panels of Fig. 10. The outcrop line perturbation is in form of (16), with $\Delta y_1 = -1.75°$. Since we will discuss the combinations of both cooling and heating, a small Δy is chosen to avoid violating the constraint discussed in Fig. 4. Due to cooling at the upper surface, the upper interface h_1 becomes shallower, with a maximum of upward displacement of 25 m, shown in the upper-left panel of Fig. 10. Both the second and the third interfaces, $h_1 + h_2$ and $h_1 + h_2 + h_3$ move downward, as shown in the middle-left and lower-left panels of Fig. 10. It is interesting to note that the third interface also moves downward, and its vertical displacement is even larger than that of the second interface. The perturbations of these two interfaces are consistent with our discussion for the two-layer model.

In this case potential vorticity isopleths in the second layer play the role of characteristics along which the signals of the cooling anomaly are advected downstream after the second layer is subducted. Therefore, the characteristic cone is defined by the streamlines or the potential vorticity isopleths in the second layer, so the outer edge of the perturbation is clearly defined by the streamlines in the second layer, as depicted by the lines with arrows. Although there is another set of characteristics, the potential vorticity isopleths in the third layer, no anomaly is propagated along these lines; thus, they play no role in setting the domain of influence.

In the second case, the model ocean is cooled along

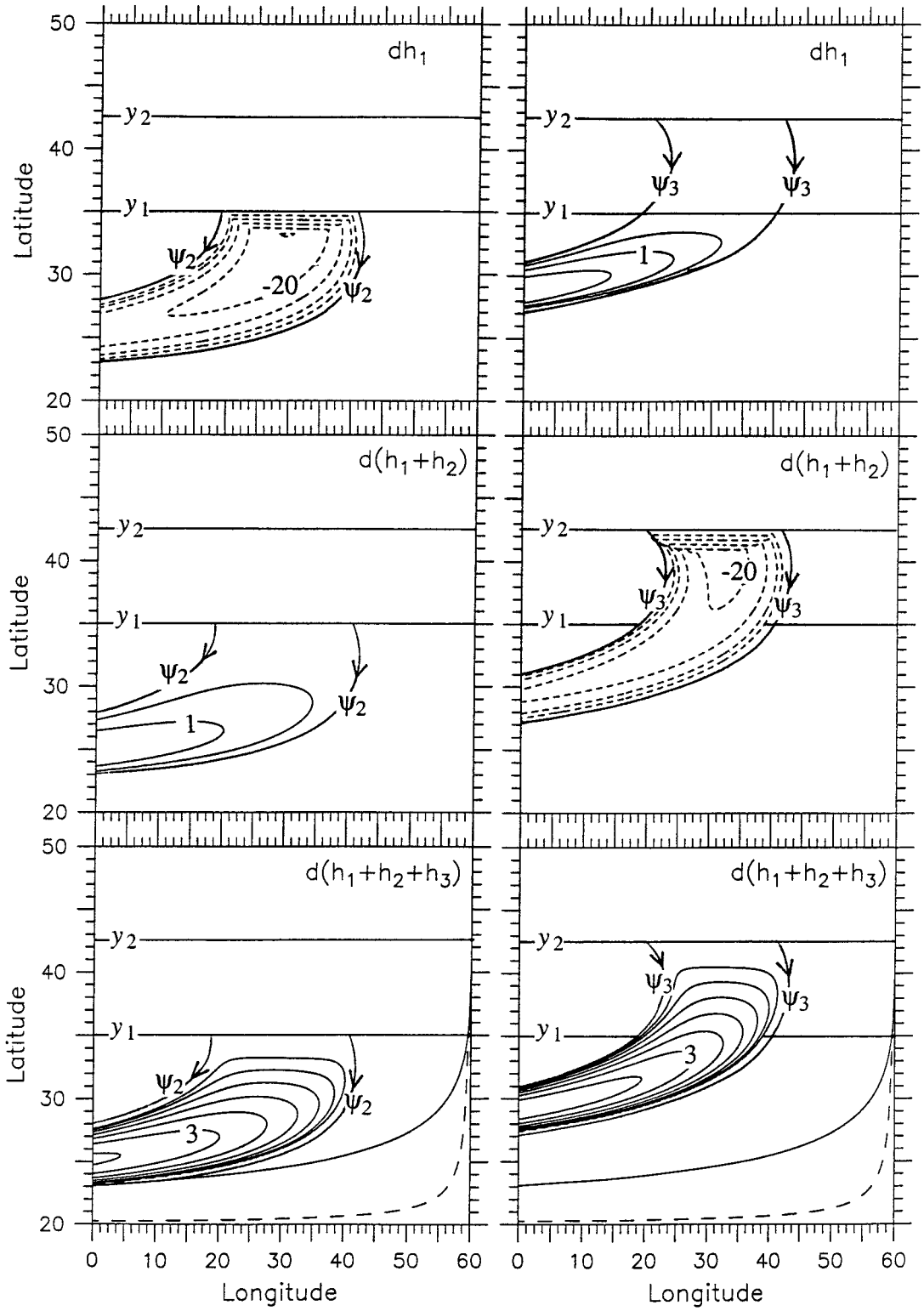

FIG. 10. Perturbations in layer thickness (m) in response to a regional cooling in a three-layer model of the ventilated thermocline. Left panels: cooling along the southern outcrop line y_1; right panels: cooling along the northern outcrop line y_1. Contour interval is 0.5 m for the positive contours and 5 m for the negative contours. Streamlines along the edge of the domain of influence in the second and third layers are depicted by lines with arrows. The solid and dashed lines near the southern edge of the basin in the lowest panels depict the shadow zone boundaries.

the northern outcrop line, with $\Delta y_2 = -1.75°$, while the southern outcrop line remains unchanged; see the right panels of Fig. 10. The second interface moves upward, with a maximum displacement of $d\ (h_1 + dh_2) = -25$ m, shown in the middle-right panel. The third interface moves downward, as discussed in the case of a two-layer model with cooling; see the lower-right panel of Fig. 10. An interesting phenomenon is the downward movement of the first interface south of the outcrop line y_1, with a maximum value of 2 m; see the upper-right panel of Fig. 10. Apparently, the upper layer becomes thicker in compensating the decline in the potential thickness of the second layer. The thickening of the upper layer due to the southward displacement of the northern outcrop line has also been confirmed by simple numerical calculations based on the LPS model, in which a uniform southward migration of the northern outcrop line induced a slightly large upper-layer thickness. However, we have not found a simple physical explanation for this phenomenon.

In this case potential vorticity isopleths in the third layer play the role of characteristics along which the signals of cooling perturbations are advected downstream after the third layer is subducted. Thus, the outer edge of the perturbation is clearly defined by the streamlines in the third layer, as depicted by the lines with arrows. Although there is another set of characteristics, the potential vorticity isopleths in the second layer, they play no role in setting up the domain of influence.

Our calculations in the case of two-layer model indicated that the difference between the fully nonlinear solutions and the solutions from the analytical solution based on the perturbation technique is relatively small, on the order of 1%–2% for $\Delta y \leq 3°$. It is interesting to note that the problem associated with the variability of the thermocline induced by climate anomaly imposed on the upper surface is of strongly nonlinear nature. Thus, perturbations induced by cooling/heating along different outcrop lines may interact with each other nonlinearly.

We present two cases to illustrate such nonlinear interactions. The parameters of the model remain the same as above. First, we carried out three experiments: case 3a in which the model ocean is cooled at y_1, with $\Delta y = -1.75°$; case 3b in which the model ocean is cooled at y_2, with $\Delta y = -1.75°$; and case 3c in which the model ocean is cooled at both y_1 and y_2, with $\Delta y = -1.75°$. The net contribution due to the nonlinear interaction is calculated by first calculating interface perturbations in these three cases, and then subtracting. For example, by subtracting dh_1 for case 3c from that for case 3a and 3b, we obtain the difference between the fully nonlinear solution and a simple linear superposition.

The nonlinear interaction between these two perturbations takes place within the area where the domains of influence of these two perturbations overlap. The boundaries of the domain of influence are defined by the streamlines in the corresponding layers, lines with arrows in the upper-left panel of Fig. 11. Even though $\Delta y = 1.75°$ is not very big, the deviation from the linear superposition is large, with a maximum amplitude roughly more than half of the perturbations themselves. The deviations from the linear superposition in the second and third interfacial displacement are also noticeable, middle-left and lower-left panels of Fig. 11.

Second, we carried out another three experiments: case 4a in which the model ocean is warmed at y_1, with $\Delta y = 1.75°$; case 4b in which the model ocean is cooled at y_2, with $\Delta y = -1.75°$; and case 4c in which the model ocean is warmed at y_1 with $\Delta y = 1.75°$ and cooled at y_2 with $\Delta y = -1.75°$. The difference between the fully nonlinear solution with these two anomalous forcing and the linear superposition of two solutions with the individual anomalous forcing is plotted on the right side of Fig. 11. A strong nonlinear interaction appears within the region where these two domains of influence overlap. Here again, the strongest nonlinear interaction appears in the upper-layer thickness.

4. Conclusions

Using the LPS model, we have examined the variability of the ventilated thermocline in response to climate changes. For simplicity, we have examined the climate changes in terms of a few idealizations: A pure cooling/heating without changes in the Ekman pumping rate and a pure change in Ekman pumping rate without changes in the outcrop line. An anomaly in thermal forcing induces a baroclinic response in the thermocline. An anomaly in Ekman pumping rate gives rise to a barotropic response. In addition, if the outcrop line is tilted, there is also a baroclinic response.

The baroclinic response of the thermocline is propagated downstream along characteristics. In the real oceans, the variability of the thermocline is a complicated combination of all these perturbations. Our studies also indicated that these perturbations are strongly nonlinear in their nature, so the climate variability due to the surface forcing anomalies may not be represented by a simple linear superposition of perturbations induced by individual forcing anomaly.

Although our simple model provides some elementary forms of the thermocline variability, the variability in the oceans is further complicated by the existence of waves that play a very important role in the geostrophic adjustment process. Recent studies, such as Deser et al. (1996) and Zhang et al. (1998), indicated that climate anomalies propagate downstream in a direction that is consistent with the ventilated thermocline theory. In addition, Liu (1999) presented interesting results from both theoretical and numerical approaches that shed light on the temporal evolution of the thermocline anomalies driven by surface forcing. Clearly, much study is required to have a better understanding of the strong nonlinear response of the thermocline to anomalous forcing.

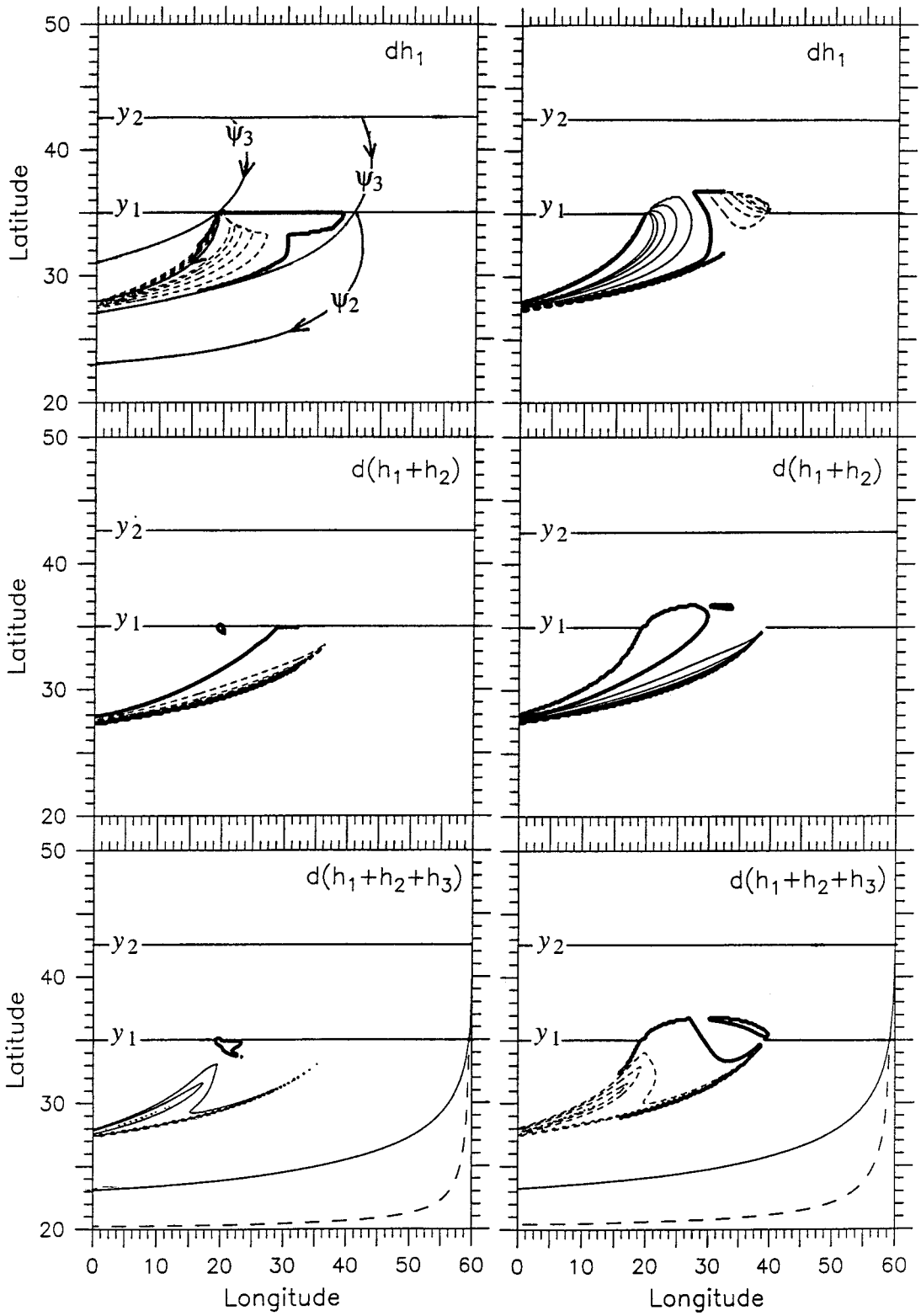

FIG. 11. Difference between a fully nonlinear solution and the linear superposition of two perturbation solutions. Left panels are for the case with cooling at both outcrop lines, and the right panels for warming along y_1 and cooling along y_2. Contour interval is 2 m for the upper panels and 0.5 m for the middle and lower panels.

Acknowledgments. During a meeting in Monterey, RXH had a brief and stimulating discussion with Dr. Ping Chang, who speculated on possible baroclinic perturbations of the thermocline in response to cold anomalies on decadal timescales. It is our great pleasure to acknowledge his initial inputs to this problem. RXH was supported by National Science Foundation through Grant OCE-9616950 to the Woods Hole Oceanographic Institution. JP was supported by National Science Foundation through Grant OCE-9301845 to the Woods Hole Oceanographic Institution.

REFERENCES

Deser, C., M. A. Alexander, and M. S. Timlin, 1996: Upper-ocean thermal variability in the North Pacific during 1970–1991. *J. Climate*, **9,** 1840–1855.

Liu, Z., 1999: Forced planetary wave response in a thermocline gyre. *J. Phys. Oceanogr.,* in press.

Luyten, J. R., J. Pedlosky, and H. Stommel, 1983: The ventilated thermocline. *J. Phys. Oceanogr.,* **13,** 292–309.

Zhang, R. H., L. M. Rostein, and A. J. Busalacchi, 1998: Origin of upper-ocean warming and El Niño change on decadal scales in the tropical Pacific Ocean. *Nature,* **391,** 879–883.